

The role of breast MR imaging in pre-operative determination of invasive disease for ductal carcinoma in situ diagnosed by needle biopsy

Mariko Goto · Sachiko Yuen · Kentaro Akazawa ·
Kaori Nishida · Eiichi Konishi · Mariko Kajihara ·
Nobuhiko Shinkura · Kei Yamada

Received: 18 July 2011 / Revised: 25 October 2011 / Accepted: 14 November 2011 / Published online: 30 December 2011
© European Society of Radiology 2011

Abstract

Objectives To evaluate whether magnetic resonance (MR) imaging features can predict the presence of occult invasion in cases of biopsy-proven pure ductal carcinoma in situ (DCIS).

Methods We retrospectively reviewed 92 biopsy-proven pure DCIS in 92 women who underwent MR imaging. The following MR imaging findings were compared between confirmed DCIS and invasive breast cancer (IBC): lesion size, type, morphological and kinetic assessments by ACR BI-RADS MRI, and findings of fat-suppressed T2-weighted (FS-T2W) imaging.

Results Sixty-eight of 92 (74%) were non-mass-like enhancements (NMLE) and 24 were mass lesions on MR imaging. Twenty-one of 68 (31%) NMLE and 13 of 24 (54%) mass lesions were confirmed as IBC. In NMLE lesions, large lesions ($P=0.007$) and higher signal intensities

(SI) on FS-T2W images ($P=0.032$) were significantly associated with IBC. Lesion size remained a significant independent predictor of invasion in multivariate analysis ($P=0.032$), and combined with FS-T2W SIs showed slightly higher observer performances (area under the curve, AUC, 0.71) than lesion size alone (AUC 0.68). There were no useful findings that enabled the differentiation of mass-type lesions.

Conclusions Breast MR imaging is potentially useful to predict the presence of occult invasion in biopsy-proven DCIS with NMLE.

Key Points

- MR mammography permits more precise lesion assessment including ductal carcinoma in situ
- A correct diagnosis of occult invasion before treatment is important for clinicians
- This study showed the potential of MR mammography to diagnose occult invasion
- Treatment and/or aggressive biopsy can be given with greater confidence
- MR mammography can lead to more appropriate management of patients

M. Goto (✉) · S. Yuen · K. Akazawa · K. Nishida · K. Yamada
Departments of Radiology, Graduate School of Medical Science,
Kyoto Prefectural University of Medicine,
465 Kajicho, Kawaramachi Hirokoji, Kamigyoku,
602-8566, Kyoto, Japan
e-mail: gomari@koto.kpu-m.ac.jp

E. Konishi
Departments of Pathology, Graduate School of Medical Science,
Kyoto Prefectural University of Medicine,
Kyoto, Japan

M. Kajihara
Departments of Radiology,
Kyoto Breast Center Sawai Memorial Clinic,
Kyoto, Japan

N. Shinkura
Departments of Surgery,
Kyoto Breast Center Sawai Memorial Clinic,
Kyoto, Japan

Keywords Breast cancer · DCIS · Occult invasion · MRI · T2-weighted image

Introduction

A diagnosis of ductal carcinoma in situ (DCIS) on needle biopsy is not infrequently followed by evidence of invasion within the final excision specimen [1–11]. Given the risk of finding invasion following a preoperative diagnosis of DCIS, there is controversy as to whether a sentinel node

procedure should be performed at the time of the initial operation [7–9, 11].

Breast magnetic resonance (MR) imaging has emerged as a highly sensitive technique for imaging breast tumours, and recently, the Breast Imaging Reporting and Data System (BI-RADS) MRI lexicon was published to overcome difficulties arising from lack of standardisation among radiologists in describing breast lesions [12]. Using the BI-RADS-MRI lexicon, DCIS can often be characterised by non-mass-like enhancements (NMLE) and exhibit segmental or ductal distribution, with clumped internal architecture [13]; however, little information in the literature describes the association between MR imaging features and the presence of occult invasion, and it seems that the BI-RADS lexicon does not perfectly describe lesions in this situation. Such preoperative differentiation of whether invasion is present is important to select the optimal treatment, and adequate diagnostic needle biopsy is needed to prevent sampling errors or underestimation in this group of lesions.

The purpose of this study was to analyse the breast MR imaging features associated with an increased risk of invasion in a group of patients with a preoperative diagnosis of DCIS on needle biopsy.

Materials and methods

Patients

From November 2008 to January 2010, 92 consecutive patients diagnosed with DCIS on needle biopsy were studied. In accordance with our institutional review board guidelines, written informed consent was obtained from all patients prior to MR examination. All were female, and their ages ranged from 29 to 86 years, with an average of 50.4 years. All 92 patients first underwent diagnostic mammography and ultrasound in our institution for their clinical problems (abnormal screening mammogram [$n=35$], palpable mass [$n=37$], discharge [$n=13$], pain [$n=6$], swelling [$n=1$]), and then MR examinations were performed before biopsy to evaluate the nature and extent of tumours detected by diagnostic mammography ($n=64$), and/or ultrasound ($n=79$). According to BI-RADS for mammography [14], 17 of the lesions were category 1, 11 were category 2, 25 were category 3, 18 were category 4 and 21 were category 5. All 17 cases of category 1, all 11 cases of category 2 and 15 cases of category 3 on mammography had abnormalities on ultrasonography (abnormal mass [$n=12$], an abnormal hypoechoic lesion [$n=26$], multiple microcysts [$n=4$], and microcalcifications in the mass [$n=1$]), and were therefore indicated for core biopsy. The other 10 cases of category 3 on mammography, which had no abnormal findings on ultrasonography, had increasing microcalcification on

follow-up mammography after 6 months, and so became candidates for stereotactic vacuum-assisted core biopsies.

Ultrasound-guided 14-gauge core biopsy (Bard Magnum Biopsy System; C.R. Bard, Covington, GA, USA) was performed in 63 patients who had an abnormality detected on ultrasonography, and 11-gauge stereotactic vacuum-assisted biopsy (Mammotome; Ethicon Endo-Surgery, Cincinnati, OH, USA) in 29 patients who showed microcalcification on mammography. The mean number of cores for each type of needle were 3.0 (range 2–7) pieces for 14-gauge core biopsy and 4.4 (range 2–10) pieces for 11-gauge vacuum-assisted biopsy.

MR protocol

MR imaging was performed with a 1.5-T system (Avanto; Siemens Medical Solutions, Erlangen, Germany). All patients were imaged in the prone position with both breasts placed into the four-channel phased array dedicated breast coil. Before administration of contrast material, a bilateral transverse fat-suppressed T2-weighted (FS-T2W) fast-spin echo sequence was performed with the following parameters: TR/TE 4,000/81 ms; field of view 32 cm; matrix size 291×256; slice thickness 5 mm with a 1-mm gap; number of excitations (NEX) 3; and time of MR data acquisition 2.3 min.

Dynamic MRI using a three-dimensional fat-suppressed volumetric interpolated breath-hold examination (VIBE) sequence with parallel acquisition was obtained before and three times after the bolus injection of Gd-DTPA (0.1 mmol/kg at a rate of 2 mL/s) followed by a 20-mL saline flush using an automatic injector (Spectris Solaris; Nihon Medrad, Osaka, Japan). Both breasts were examined in the transverse plane on the first-, second- and third-phase dynamic images acquired at 60 s, 130 s and 380 s, respectively. The dynamic MRI parameters were as follows: TR/TE/FA 4.7/2.4/15 ms; field of view 32 cm; matrix 384×384; interpolated slice thickness 1 mm; time of acquisition 70 s. The right and left breasts were examined sagittally using the VIBE sequence without parallel acquisition at 200 and 290 s; that is, between the second- and third-phase dynamic images, respectively (TR/TE/FA, 5.2/2.4/12 ms; field of view 17 cm; matrix 256×256; interpolated slice thickness 0.7 mm; time of acquisition 90 s). Maximum intensity projection and coronal multiplanar reconstruction were performed on the MRI console for visualisation of the extent of breast cancer using second-phase dynamic images.

Image interpretation

All MR images were posted on the PACS (picture archiving and communication system) workstation (Siemens Medical Solutions, Erlangen, Germany) for review by radiologists.

MR images of invasive breast cancers (IBC) and pure DCIS were randomised and independently reviewed using the BI-RADS MR lexicon [12] by two radiologists (M.G. and S.Y., with 8 and 13 years of breast MR imaging experience, respectively). The only information available at the time of evaluation, apart from the breast of interest, was that a histologically verified lesion had been previously described for the breast. If different BI-RADS assessment categories were assigned by the two readers, a consensus was reached after discussion of the findings. Using the BI-RADS MR lexicon, the morphology and kinetics on MR imaging were evaluated for all enhancing lesions, and concurrently, we recorded the enhancing lesion size.

For the time-signal intensity curves, one of the authors (M.G.) placed regions of interest (ROI) using dynamic images on an interactive workstation (Aquarius; Tera Recon Inc., CA, USA) to evaluate the enhancement pattern that demonstrated higher visual enhancement. Time-signal intensity curve patterns were categorised into three types for the initial rise (fast, medium, slow) and the delayed phase (persistent, plateau, washout).

In addition, on the FS-T2W images, we evaluated the signal intensity (SI) of the detected enhancing lesions, referring to the dynamic MR images. Qualitative assessment based on visual evaluation determined whether the SI of the lesion was relatively lower than, higher than, or indistinctive from that of the surrounding or contralateral normal breast tissue. Quantitative assessment was performed by obtaining ROI measurements of lesion SI and contralateral normal breast tissue SI. The lesion SI ratio was calculated by dividing lesion SI by normal breast tissue SI: (lesion SI/normal breast tissue SI).

Histopathological analysis

The core biopsy specimens were formalin-fixed, paraffin-embedded, and processed according to the standard protocol. Each biopsy was stained with haematoxylin and eosin for histological examination. Surgical samples for histopathological examinations were prepared by making serial 5-mm slices of breast-conserving surgical specimens and 5–10 mm slices of mastectomy specimens. Histological diagnoses were made by one author who is an expert in breast pathology (E.K., with 10 years of experience in breast histological evaluation), and the following histological features were recorded: the subtype of DCIS (comedo or non-comedo) and nuclear grade (1, 2 or 3) from core biopsy samples, and the presence or absence of invasive tumours, the size and number of invasive nests and the percentage of DCIS in the lesion from final surgical specimens.

Statistical analysis

The patients' characteristics, histological characteristics and MR imaging findings were compared in each group using the Chi-square (χ^2) or Fisher's exact test if the data were qualitative, and by the Wilcoxon rank-sum test or Student's *t*-test if the characteristics were quantitative. Factors that were significantly associated with outcome on univariate analysis were entered together into multivariate analysis using logistic regression model, and operating characteristics to discriminate IBC and DCIS were examined using receiver operating characteristic (ROC) curves. All statistical analyses were performed using JMP 9.0 (SAS Japan, Tokyo, Japan). A *P* value of less than 0.05 was considered to indicate a statistically significant difference.

Results

Subjects and lesions

The study included 92 patients with 92 lesions of biopsy-proven pure DCIS. All patients underwent surgery at our institute without neoadjuvant chemotherapy, and IBC was found in 34/92 (37%) cases (14-gauge core biopsy; 30/63 [48%], 11-gauge vacuum-assisted biopsy; 4/29 [14%]), and the remaining 58 were histopathologically shown to be pure DCIS. Comparative clinicopathological data of the IBC and pure DCIS are summarised in Table 1. There were no statistically significant differences in patient age, nuclear grade of the tumour and DCIS subtype on core biopsy specimens.

Sixty-seven (73%) patients underwent breast-conserving surgery and 25 (27%) underwent mastectomy. Sentinel lymph node biopsy was performed in 86 (93%) patients,

Table 1 Characteristics of patients and core biopsy pathology with IBC and those with pure DCIS

Characteristic	IBC (<i>n</i> =34)	DCIS (<i>n</i> =58)	<i>P</i> value
Age (years) ^a	54 (32–83)	49 (29–86)	0.062
Nuclear grade			
1	3 (9)	6 (10)	0.493
2	23 (68)	44 (76)	
3	8 (23)	8 (14)	
DCIS subtype			
Comedo	15 (44)	33 (57)	0.283
Non-comedo	19 (56)	25 (43)	

Unless otherwise indicated, data are numbers of patients, with percentages in parentheses

IBC invasive breast cancer. DCIS ductal carcinoma in situ

^aData are the means, with ranges in parentheses

Table 2 Comparison of histological findings between mass and NMLE lesion on MR images

Histological findings	Mass (n=24)	NMLE (n=68)	P value
Histological type			
Ductal carcinoma in situ	11 (46)	47 (69)	0.052
Invasive breast cancer	13 (54)	21 (31)	
Invasive ductal carcinoma	13 (100)	18 (86)	
Invasive lobular carcinoma	0	2 (10)	
Mucinous carcinoma	0	1 (5)	
Percentage of DCIS			
100% (Pure DCIS)	11 (46)	47 (69)	0.003
≥75%	3 (13)	18 (26)	
≥50%	6 (25)	2 (3)	
≥25%	2 (8)	1 (1.5)	
≥0%	2 (8)	0	
Size of invasive nest (mm) ^a	17 (0.5–100)	7 (0.5–35)	0.123
Number of invasive nests			
0	11 (46)	47 (69)	0.105
1	13 (54)	15 (22)	
2	0	3 (4.5)	
≥3	0	3 (4.5)	

Unless otherwise indicated, data are numbers of patients, with percentages in parentheses

NMLE non-mass-like enhancement lesion. DCIS ductal carcinoma in situ

^aData are the means, with ranges in parentheses

except for 6 patients who had been diagnosed as having only a very limited extent of tumour. Four of 86 patients (5%) were found to have sentinel lymph node metastases and subsequently underwent axillary dissection. After initial surgery, two of the 67 (3%) breast-conserving patients underwent mastectomy because of a positive margin for an intraductal malignant component.

Correlation between MR imaging and histological features

On MR images, 68 of 92 (74%) lesions were depicted as NMLE lesion types, and the remaining 24 lesions were depicted as mass lesion types. Table 2 shows the histological findings of each mass and NMLE lesion on MR images and Table 3 shows MR imaging findings of each IBC and DCIS. DCIS most commonly showed NMLE on MR (81% [47 of 58], Fig. 1); however, many IBC also exhibited NMLE (62% [21 of 34], Fig. 2), and there were no statistically significant differences between IBC and DCIS in the lesion type ($P=0.052$). Enhancing lesion size ($P=0.013$) and FS-T2W imaging findings ($P=0.007$) showed statistically significant differences between IBC and DCIS (Table 3), and on the quantitative assessment in FS-T2W imaging, the mean lesion T2 SI ratios of IBC (mean $1.50 \pm SD 0.60$) were significantly higher than those of pure DCIS (mean $1.23 \pm SD 0.36$) ($P=0.023$).

Lesions with a higher percentage of DCIS tended to show NMLE on MR images with a statistically significant difference (Table 2: $P=0.003$), and other histological findings, and the size and number of invasive nests, had no

association with the lesion type on MR images. There was also no statistically significant association between histological DCIS features and enhancing lesion size or FS-T2W imaging findings on MR images.

MR imaging findings of mass lesion type

In the 24 lesions that were depicted as mass lesion types on MR images, 13 (54%) were IBC (Fig. 3) and 11 were DCIS. There were no statistically significant differences in the MR imaging findings between IBC and DCIS in the mass lesion

Table 3 Comparison of MR imaging findings between patients with IBC and patients with pure DCIS

MR imaging finding	IBC (n=34)	DCIS (n=58)	P value
Lesion size (mm) ^a	41(15–88)	30(8–90)	0.013
Lesion type			
Mass	13 (38)	11 (19)	0.052
Non-MassLike enhancement	21 (62)	47 (81)	
Signal intensity of the enhancing lesion on FS-T2W image			
Higher	22 (65)	22 (38)	0.007
Lower	4 (12)	3 (5)	
Indistinctive	8 (24)	33 (57)	

Unless otherwise indicated, data are numbers of patients, with percentages in parentheses

IBC invasive breast carcinoma. DCIS ductal carcinoma in situ

FS-T2W fat-suppressed T2-weighted

^aData are the means, with ranges in parentheses

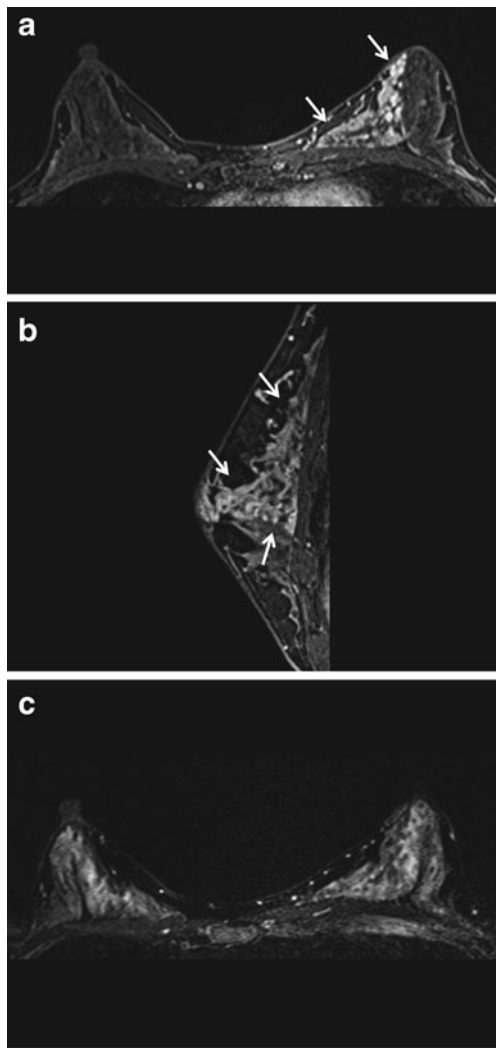


Fig. 1 A 46-year-old woman with ductal carcinoma in situ (DCIS) in the left breast. **a** Axial contrast-enhanced image obtained 130 s after the administration of intravenous contrast material showed non-mass-like, segmental enhancement in the left breast (*arrows*). **b** Sagittal contrast-enhanced image obtained 200 s after the administration of contrast material showed confluent segmental enhancement composed of heterogeneous enhancement (*arrows*). **c** Axial T2-weighted image with fat suppression could not distinguish the enhancing lesion from background normal breast tissue as an abnormal intensity area. Lesion signal intensity ratio was 0.95

types (Table 4). In contrast to pure DCIS, IBC tended to be larger on MR images, but this difference was not statistically significant ($P=0.079$). On the FS-T2W image, while 13 of all IBC could be detected as relatively lower ($n=4$) (Fig. 3) or higher ($n=9$) SI, two of 11 DCIS (18%) were indistinct from normal breast tissue; however, there were no statistical significant differences between IBC and DCIS in the findings on FS-T2W images ($P=0.273$). Similarly, using quantitative assessment, the mean lesion T2 SI ratios of IBC (mean $1.43 \pm$ SD 0.63) were not significantly different from those of pure DCIS (mean $1.29 \pm$ SD 0.40, $P=0.487$, Fig. 4).

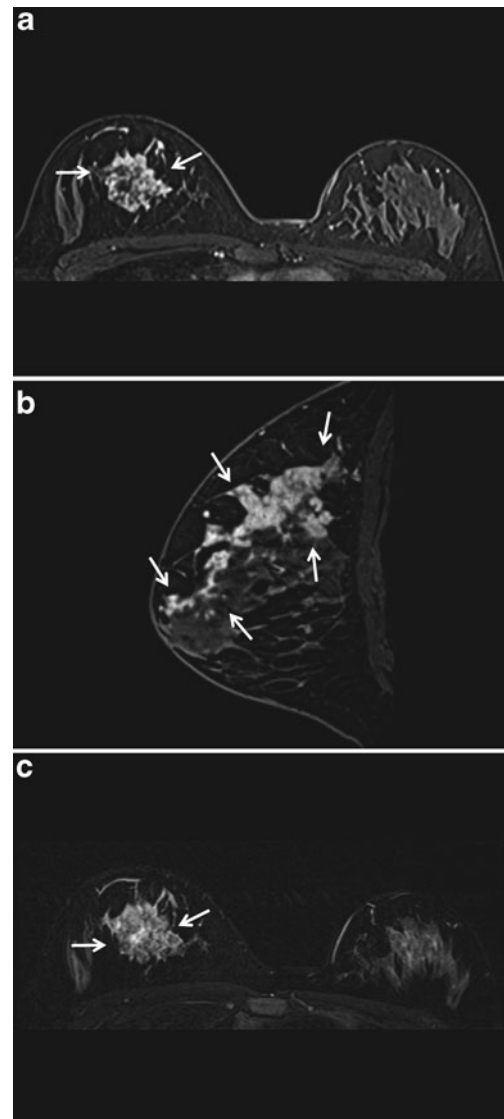


Fig. 2 A 29-year-old woman with invasive ductal carcinoma in the right breast. **a** Axial contrast-enhanced image obtained 130 s after the intravenous administration of contrast material showed non-mass-like enhancement lesion (*arrows*). **b** Sagittal contrast-enhanced image obtained 200 s after the administration of contrast material showed confluent segmental enhancement composed of heterogeneous enhancement (*arrows*). **c** Axial T2-weighted image with fat suppression showed high-signal intensity of the enhancing lesion compared with surrounding or contralateral normal breast tissue. Lesion signal intensity ratio was 1.67

MR imaging findings of non-mass-like enhancement lesion type

In the 68 lesions that were depicted as NMLE lesion types on MR images, 21 were IBC and 47 (69%) were DCIS. Regarding the contrast-enhancement morphological features and kinetic descriptor on MR images, there were no statistical significant differences between IBC and DCIS (Table 5). On the FS-T2W images, while 13 of 21 (62%) IBC could be

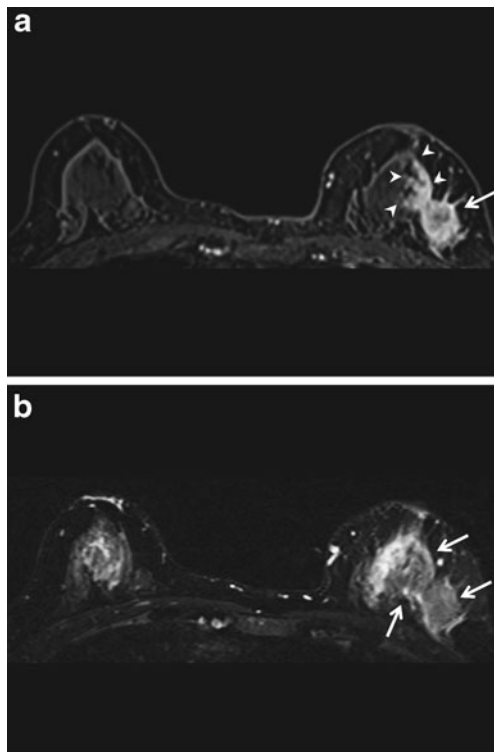


Fig. 3 A 52-year-old woman with invasive ductal carcinoma in the left breast. **a** Axial contrast-enhanced image obtained 130 s after the intravenous administration of contrast material showed an irregular mass lesion (*arrow*) associated with a non-mass-like enhancement area in the direction of the nipple (*arrowheads*). **b** Axial T2-weighted image with fat suppression showed a low-signal intensity mass and area compared with surrounding or contralateral normal breast tissue. Lesion signal intensity ratio was 0.71

detected as lesions with higher SI (Fig. 2), only 16 of 47 (34%) DCIS could be detected as higher SI. No lesions were detected as lower SI in either IBC or DCIS groups. Thirty-one of 47 (66%) DCIS were indistinct (Fig. 1), and findings on FS-T2W images between DCIS and IBC showed statistically significant differences ($P=0.032$). Quantitative assessment also showed a higher T2 SI ratio for IBC (mean $1.47 \pm \text{SD } 0.48$) than pure DCIS (mean $1.22 \pm \text{SD } 0.35$) with statistical significance ($P=0.035$, Fig. 4). All eight IBC that could not be detected on FS-T2W images had a high percentage of DCIS within the lesion (all $\geq 75\%$ DCIS), and had a smaller invasive nest than lesions detected as higher SI on FS-T2W images with statistically significant differences (Table 6, $P=0.018$).

In addition, the enhancing lesion size on MR images of IBC was larger than DCIS with a statistically significant difference (Table 5, $P=0.007$). On multivariate analysis, lesion size also remained a significant independent predictor of invasion ($P=0.032$). The area under the curve (AUC) of ROC analysis was 0.68 and was slightly improved by combining FS-T2W imaging findings (AUC=0.71) for discriminating IBC from DCIS (Fig. 5).

Table 4 Comparison of MR imaging findings in mass lesion type between patients with IBC and patients with pure DCIS

AR imaging finding	IBC ($n=13$)	DCIS ($n=11$)	P value
Lesion size (mm) ^a	31 (15–80)	18 (8–30)	0.079
Mass shape			
Round/Oval	0	0	1.000
Lobulated	1 (8)	0	
Irregular	12 (92)	11 (100)	
Mass margin			
Smooth	3 (23)	2 (18)	1.000
Irregular	10 (77)	9 (82)	
Spiculated	0	0	
Internal enhancement			
Homogeneous	1 (8)	1 (9)	0.817
Heterogeneous	8 (62)	8 (73)	
Rim	4 (30)	2 (18)	
Initial phase enhancement kinetic descriptor			
Fast	12 (92)	11 (100)	1.000
Medium	1 (8)	0	
Slow	0	0	
Delayed phase enhancement kinetic descriptor			
Persistent	4 (30)	4 (36)	0.625
Plateau	1 (8)	2 (18)	
Washout	8 (62)	5 (46)	
Signal intensity of the enhancing lesion on FS-T2W image			
Higher	9 (69)	6 (55)	0.273
Lower	4 (31)	3 (27)	
Indistinctive	0	2 (18)	

Unless otherwise indicated, data are numbers of patients, with percentages in a parentheses

IBC invasive breast carcinoma. DCIS ductal carcinoma in situ

FS-T2W fat-suppressed T2-weighted

^aData are the means, with ranges in parentheses

Discussion

Our study results showed that several MR imaging findings of breast lesions, especially in NMLE-type lesions, such as a large enhancing lesion and lesion detection with relatively higher SI on FS-T2W images, are suggestive of invasion in biopsy-proven DCIS. On the other hand, it was confirmed that findings according to BI-RADS MRI are not useful for differentiation between IBC and DCIS, and that there is virtually no imaging clue that differentiates IBC from pure DCIS in mass-type lesions.

Preoperative identification of invasion in malignant disease of the breast is important because lymph node staging procedures are required in invasive disease. In the present study, 37% of patients with the initial diagnosis of DCIS had invasive disease on final specimen histology, and this is comparable with other recent studies with invasion rates of between 14% and 44% [1–11]. Hence, some previous investigators

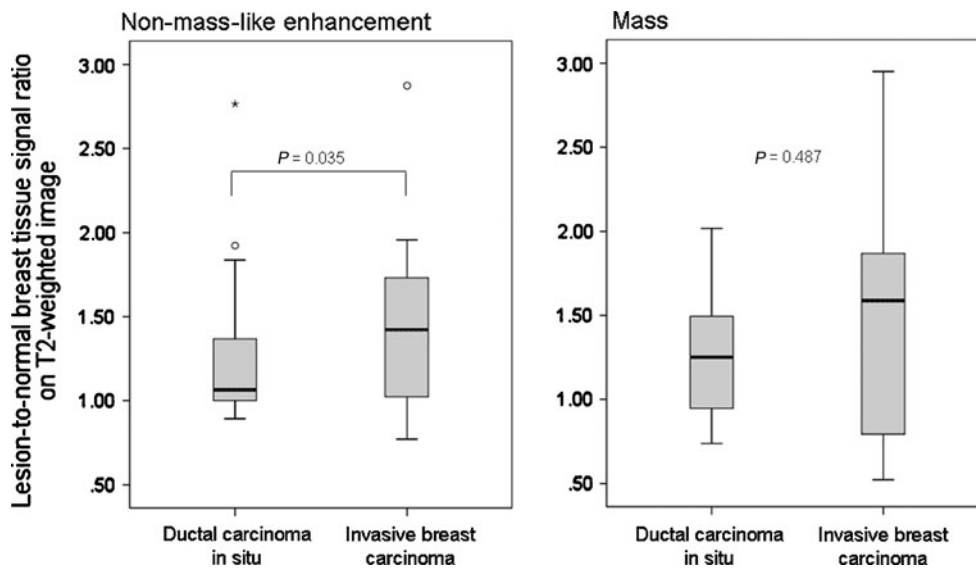


Fig. 4 Graph shows lesion-to-normal breast tissue signal intensity ratios on fat-suppressed T2-weighted images by each type of lesion. The mean value of the signal ratio was statistically significantly higher

in invasive carcinoma than ductal carcinoma in situ on non-mass-like enhancement ($P=0.035$), however, there was no statistical significance for the mass lesion ($P=0.487$)

tried to identify histological risk factors from biopsy specimens that are associated with invasive disease [1, 4–9, 11]. Some of these reports indicated that a high nuclear grade [5–7] or the existence of comedo necrosis [1, 7] on core biopsy specimens suggested the presence of an invasive nest; however, in other studies, the results seem controversial [1, 4, 8, 9, 11] including our study (Table 1). The core biopsy specimen represents only part of the whole tumour, and thus predicting the histological features of the tumour would be difficult, leading to widely varying results among studies.

Therefore, some researchers insist on using a thicker needle with a vacuum system to gather more specimens to collect the invasion focus in the biopsy specimen [2, 4, 7]. Also in our study, patients with 11-gauge stereotactic vacuum-assisted biopsy showed a lower underestimation rate (14%) than patients with 14-gauge core biopsy (48%). Using a larger needle and/or vacuum-assisted technique may be an effective procedure for decreasing the underestimation of IBC but, on the other hand, it will increase physical invasion for the patients. Therefore, an additional less-invasive technique is required for the assessment of occult invasion before a more aggressive biopsy or a surgical procedure.

Breast MR imaging is a less-invasive technique and is now widely accepted as a tool for clinical workup. There has been some controversial discussion about the diagnostic performance of breast MR imaging for DCIS [15]; however, recent advances in high-spatial resolution or diffusion-weighted imaging have been reported to be useful for the detection and staging of DCIS in comparison with other conventional imaging [16–18]. Thus, breast MR imaging should have a potential role in diagnosing the accurate extent of the occult invasion of DCIS; however, previously, there have been only

a few extensive discussions about which MR findings are most related to the presence of occult invasion.

According to the recently published BI-RADS MRI lexicon [12], lesion configuration, classified as either mass enhancement or NMLE, should be determined first. Typically, it has been described that IBC tended to be classified as the mass lesion type, and pure DCIS as NMLE (60–80%) [13, 19, 20]. In our study, 81% of pure DCIS showed NMLE; however, many IBC (21 of 34: 62%) were also included in the NMLE type reflecting an abundant intraductal component (Table 2, $P=0.003$), and there was no statistically significant differences in lesion types between IBC and pure DCIS (Tables 2, 3: $P=0.052$). MR imaging findings with statistically significant differences between IBC and DCIS were enhancing lesion size ($P=0.013$) and findings of FS-T2W imaging ($P=0.007$).

For assessment by each lesion type, in the NMLE lesion, no morphological or kinetic findings could differentiate IBC from pure DCIS according to BI-RADS MRI classification in our study (Table 5). The most frequent morphological descriptor of NMLE DCIS was segmental (59%), but this was also true for IBC (71%). On contrast-enhancement MR images, segmental enhancement has been reported not only in DCIS, but also in IBC [21]. This may have occurred because of the difficulty in differentiating invasive foci from the surrounding non-mass-like enhancement that reflects the DCIS component, and we suppose that this is one reason why it is difficult to differentiate IBC with an abundant DCIS component from pure DCIS. Also, in kinetic curve assessments, lesions with an abundant intraductal component have been reported not to show typical malignant enhancement patterns [22–24].

Table 5 Comparison of MR imaging findings in NMLE lesion type between patients with IBC and patients with pure DCIS

MR imaging finding	IBC (n=21)	DCIS (n=47)	P value
Lesion size (mm) ^a	48 (16–88)	32 (8–90)	0.007*
Non-mass descriptor			
Segmental	15 (71)	28 (59)	0.804
Linear/Ductal	2 (10)	6 (13)	
Focal	4 (19)	7 (15)	
Regional	0	1 (2)	
Multiple regions	0	1 (2)	
Diffuse	0	4 (9)	
Internal enhancement			
Homogeneous	2 (10)	5 (11)	0.924
Heterogeneous	16 (76)	37 (79)	
Clumped	3 (14)	4 (9)	
Punctate	0	1 (2)	
Initial phase enhancement kinetic descriptor			
Fast	15 (71)	23 (49)	0.260
Medium	2 (9.5)	7 (15)	
Slow	4 (19)	17 (36)	
Delayed phase enhancement kinetic descriptor			
Persistent	8 (38)	30 (64)	0.110
Plateau	11 (52)	15 (32)	
Washout	2 (10)	2 (4)	
Signal intensity of the enhancing lesion on ES T2W image			
Higher	13(62)	16 (34)	0.032
Lower	0	0	
Indistinctive	8 (38)	31 (66)	

Unless otherwise indicated, data are numbers of patients, with percentages in parentheses

NMLE non-masslike enhancement. IBC invasive breast carcinoma. DCIS ductal carcinoma in situ

FS-T2W fat-suppressed T2-weighted

^aData are the means, with ranges in parentheses

*Variable with significant difference also shown by multivariate analysis ($P=0.032$)

Table 6 Comparison of histological findings between higher SI and indistinctive lesion on FS-T2W images in NMLE lesion

Histological findings	Higher SI (n=13)	Indistinctive (n=8)	P value
Size of invasive nest (mm) ^a	10 (0.5–35)	1.5 (0.3–4)	0.018
Percentage of \geq DCIS 75%	10 (77)	8 (100)	0.257
Multiple invasive nests	3 (23)	3 (38)	0.631

Unless otherwise indicated, data are numbers of patients, with percentages in parentheses

SI signal intensity. FS-T2W fat-suppressed T2-weighted

NMLE non-masslike enhancement. DCIS ductal carcinoma in situ

^aData are the means, with ranges in parentheses

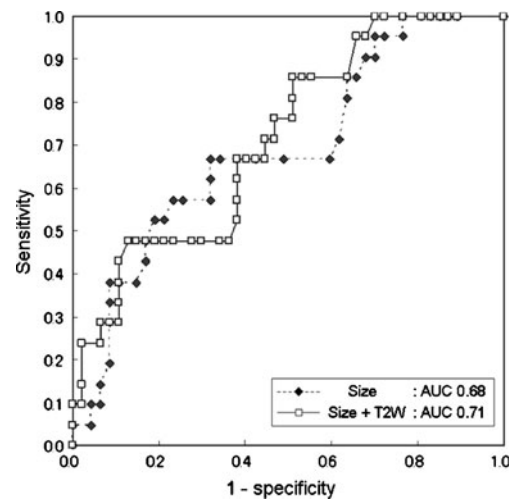


Fig. 5 Receiver operating characteristics curves for enhancing lesion size (dashed line with solid diamond) and combination of lesion size and T2-weighted (T2W) signal (solid line with open square) in non-mass-like enhancement. Difference in area under curve (AUC) was not statistically significant ($P=0.807$); however, the AUC was slightly improved by combining the T2W signal finding

FS-T2W imaging was useful to differentiate DCIS from IBC in the NMLE lesion type in our study. Relatively higher SI on FS-T2W imaging, which corresponds to the enhancing lesion on dynamic MR imaging, was present in 62% (13 of 21) of patients with invasion (Fig. 2) and was absent in 66% (31 of 47) of patients without invasive tumours (Fig. 1), and these differences were statistically significant ($P=0.032$). This result was also confirmed by quantitative assessment (Fig. 4, $P=0.035$). IBC that could be detected by FS-T2W imaging had a significantly larger invasive nest than lesions which could not be detected (Table 6, $P=0.018$). Eight IBCs that could not be detected on FS-T2W images all had only small invasive nests (≤ 4 mm). Yuen et al [25] reported that surrounding high SI of the enhancing lesion on T2-weighted images was a clue to the diagnosis of invasive cancer for segmental enhancing lesions on MR images. It may be that the patient's immune system mounts an inflammatory response to the tumour once invasion occurs and, in some previous reports, inflammatory cell infiltration in core biopsy specimens was depicted as an invasive nest [4, 6]. FS-T2W imaging was sensitive to the presence of minute amounts of fluid or edema, and we suppose that these histopathological characteristics were reflected in this imaging finding. We believe that a larger invasive focus hidden by segmental enhancement on the contrast-enhanced image could be depicted on FS-T2W images as higher SI of the lesion.

On the other hand, 34% of NMLE-type pure DCIS showed higher SI on FS-T2W images and, for this reason, this finding had a low positive predictive value (16 of 29: 45%). In some reports, pure DCIS was occasionally accompanied by periductal inflammatory cell infiltration [4, 6, 11], and these desmoplastic changes may be reflected as higher

SI in DCIS on FS-T2W images. Other possible reasons could be dilated ducts or multiple microcysts; however, 66% of pure DCIS were undifferentiated from normal breast tissue on FS-T2W images in our study, and FS-T2W images finally showed a high negative predictive value for IBC on NMLE type (31 of 39: 79%). We thus believe that this information obtained from FS-T2W images is important as a clue for predicting the invasion of biopsy-proven DCIS.

Lesion size on contrast-enhanced MR images was useful for predicting IBC in NMLE lesions, with statistically significant differences in both univariate ($P=0.007$) and multivariate ($P=0.032$) analysis (Table 5). In the analysis of mammographical features of patients with DCIS on core biopsy, the presence of a mass and large extension of calcification increased the risk of the presence of invasion [3, 6, 7, 9, 10, 26]. In addition, also in the analysis of histological factors, a large DCIS lesion was described to be associated with invasion [1, 2]. In the DCIS, MR imaging was reportedly more sensitive for detection of the lesion, with higher accuracy for determining the extent of disease than mammography [15, 27, 28]. Thus, to estimate histological lesion size, overall, MR imaging was more reliable than mammography. It is important that MR images can depict the lesion size more accurately because it is considered more useful and reliable to predict occult invasion than mammography. In ROC analysis, AUC of the enhancing lesion size for discriminating IBC was 0.68, and by combining with the FS-T2W imaging finding, the AUC slightly improved (0.71, Fig. 5). When higher SI on FS-T2W imaging and/or a large enhancing lesion were demonstrated on MR imaging, more aggressive biopsy using a larger needle and/or a vacuum-assisted technique should be considered before surgical excision of NMLE lesions.

In the mass-lesion-type, no clue enabled differentiation of the IBC from pure DCIS, including the enhancing lesion size and FS-T2W image. On FS-T2W images, two undetectable lesions were both pure DCIS; however, there was no statistical difference between DCIS and IBC (Table 4). As a result, there were no imaging clues as to how to differentiate DCIS from IBC in mass-lesion-types; however, given that more than half of the lesions (54%) were IBC, a mass lesion on the MR image should be planned for surgical operation as an invasive lesion, including sentinel lymph node biopsy in spite of the biopsy result.

This study had several limitations. First, the number of patients studied was small; therefore, the statistical significance of these findings may be insufficient. Further validation in a larger study population is thus warranted. Second, we did not correlate the findings with patients' menstrual status or cycle. This menstrual status could have possibly influenced the normal breast parenchymal intensity on T2-weighted images and enhancement; therefore, we cannot exclude the possibility that our visual assessment was influenced by the condition of normal breast tissue.

In conclusion, MR imaging seems unable to differentiate between IBC and pure DCIS according to BI-RADS MRI classification, on morphological or kinetic grounds. However in the NMLE lesion type, a large enhancing lesion and higher SI on FS-T2W images were predictive risk factors of invasive disease. By comparison, the mass-lesion-type did not demonstrate any effective imaging markers to predict the invasive risk and thus all such lesions should be managed as invasive disease.

References

1. Renshaw AA (2002) Predicting invasion in the excision specimen from core needle biopsy specimens with only ductal carcinoma in situ. *Arch Pathol Lab Med* 126:39–41
2. Jackman RJ, Burbank F, Parker SH (2001) Stereotactic breast biopsy of non palpable lesions: determinants of ductal carcinoma in situ underestimation rates. *Radiology* 218:497–502
3. Lagios MD, Westdahl PR, Margolin FR, Rose MR (1982) Duct carcinoma in situ. Relationship if extent of non-invasive disease to the frequency of occult invasion, multicentricity, lymph node metastases, and short term treatment failures. *Cancer* 50:1309–1314
4. Lee CH, Carter D, Philpotts LE et al (2000) Ductal carcinoma in situ diagnosed with stereotactic core needle biopsy: can invasion be predicted? *Radiology* 217:466–470
5. Bonnett M, Wallis T, Rossmann M et al (2002) Histological and radiological analysis of ductal carcinoma in situ diagnosed stereotactic incisional core breast biopsy. *Mod Pathol* 15:95–101
6. Hoorntje LE, Schipper ME, Peeters PH et al (2003) The findings of invasive cancer after a preoperative diagnosis of ductal carcinoma in situ: causes of ductal carcinoma in situ underestimates with stereotactic 14-gauge needle biopsy. *Ann Surg Oncol* 10:748–753
7. Yen TW, Hunt KK, Ross MI et al (2005) Predictors of invasive breast cancer in patients with an initial diagnosis of ductal carcinoma in situ: a guide to selective use of sentinel lymph node biopsy in management of ductal carcinoma in situ. *J Am Coll Surg* 200:516–526
8. Mittendorf EA, Arciero CA, Gutchell V, Hooke J, Shriver CD (2005) Core biopsy diagnosis of ductal carcinoma in situ: an indication for sentinel lymph node biopsy. *Curr Surg* 62:253–257
9. Goyal A, Douglas-Jones A, Monypenny I et al (2006) Is there a role of sentinel lymph node biopsy in ductal carcinoma in situ? Analysis of 587 cases. *Breast Canc Res Treat* 98:311–314
10. Dillon MF, McDermott EW, Quinn CM et al (2006) Predictors of invasive disease in breast cancer when core biopsy demonstrates DCIS only. *J Surg Oncol* 93:559–563
11. Huo L, Sneige N, Hunt KK, Albarracin CT, Lopez A, Resetskova E (2006) Predictors of invasion in patients with core-needle biopsy-diagnosed ductal carcinoma in situ and recommendations for a selective approach to sentinel lymph node biopsy in ductal carcinoma in situ. *Cancer* 107:1760–1768
12. American College of Radiology (2003) Breast Imaging Reporting and Data System (BI-RADS)—MRI atlas, 1st edn. American College of Radiology, Reston
13. Jansen SA, Newstead GM, Abe H et al (2007) Pure ductal carcinoma in situ: kinetic and morphologic MR characteristics compared with mammographic appearance and nuclear grade. *Radiology* 245:684–691
14. American College of Radiology (2003) Breast Imaging Reporting and Data System (BI-RADS)—mammography atlas, 4th edn. American College of Radiology, Reston

15. Schouten van der Velden AP, Schlooz-Vries MS, Boetes C, Wobbes T (2009) Magnetic resonance imaging of ductal carcinoma in situ: what is its clinical application? A review. *Am J Surg* 198:262–269
16. Berg WA, Gutierrez L, NessAiver MS et al (2004) Diagnostic accuracy of mammography, clinical examination, US, and MR imaging in preoperative assessment of breast cancer. *Radiology* 233:830–849
17. Kuhl CK, Schrading S, Bieling HB et al (2007) MRI for diagnosis of pure ductal carcinoma in situ: a prospective observational study. *Lancet* 370:485–492
18. Rahbar H, Partridge SC, Eby PR et al (2011) Characterization of ductal carcinoma in situ on diffusion weighted breast MRI. *Eur Radiol* 21:2011–2019
19. Rosen EL, Smith-Foley SA, DeMartini WB, Eby PR, Peacock S, Lehman CD (2007) BI-RADS MRI enhancement characteristics of ductal carcinoma in situ. *Breast J* 13:545–550
20. Menell JH, Morris EA, Dershaw DD, Abramson AF, Brogi E, Liberman L (2005) Determination of the presence and extent of pure ductal carcinoma in situ by mammography and magnetic resonance imaging. *Breast J* 11:382–390
21. Kuhl C (2007) The current status of breast MR imaging. Part I. Choice of technique, image interpretation, diagnostic accuracy, and transfer to clinical practice. *Radiology* 244:356–378
22. Facius M, Renz DM, Neubauer H et al (2007) Characteristics of ductal carcinoma in situ in magnetic resonance imaging. *Clin Imag* 31:394–400
23. Kuhl C (2006) Concepts for differential diagnosis in breast MR imaging. *Magn Reson Imag Clin N Am* 14:305–328
24. Yuen S, Uematsu T, Masako K, Uchida Y, Nishimura T (2008) Segmental enhancement on breast MR images: differential diagnosis and diagnostic strategy. *Eur Radiol* 18:2067–2075
25. Yuen S, Uematsu T, Kasami M, Tanaka K, Kimura K, Sanuki J, Uchida Y, Furukawa H (2007) Breast carcinomas with strong high-signal intensity on T2-weighted MR images: pathological characteristics and differential diagnosis. *J Magn Reson Imaging* 25:502–510
26. Stomper PC, Geradts J, Edge SB, Levine EG (2003) Mammographic predictors of the presence and size of invasive carcinomas associated with malignant microcalcification lesions without a mass. *Am J Roentgenol* 181:1679–1684
27. Uematsu T, Yuen S, Kasami M, Uchida Y (2008) Comparison of magnetic resonance imaging, multidetector row computed tomography, ultrasonography, and mammography for tumour extension of breast cancer. *Breast Canc Res Treat* 112:461–474
28. Marcotte-Bloch C, Balu-Maestro C, Chamorey E, Ettore F, Raoust I, Flipo B, Chapellier C (2011) MRI for the size assessment of pure ductal carcinoma in situ (DCIS): a prospective study of 33 patients. *Eur J Radiol* 77:462–467